Neuroelectrophysiology-Compatible Electrolytic Lesioning

Iliana E. Bray[1†], Stephen E. Clarke[2†], Kerriann Casey[3], Paul Nuyujukian[2,4,1,5,6*], for the Brain Interfacing Laboratory[2]

***For correspondence:** (PN)

[†]These authors contributed equally to this work

[1]Department of Electrical Engineering; [2]Department of Bioengineering; [3]Department of Comparative Medicine; [4]Department of Neurosurgery; [5]Wu Tsai Neuroscience Institute; [6]Bio-X, Stanford University, United States

Abstract Lesion studies have historically been instrumental for establishing causal connections between brain and behavior. They stand to provide additional insight if integrated with multielectrode techniques common in systems neuroscience. Here we present and test a platform for creating electrolytic lesions through chronically implanted, intracortical multielectrode probes without compromising the ability to acquire neuroelectrophysiology. A custom-built current source provides stable current and allows for controlled, repeatable lesions in awake-behaving animals. Performance of this novel lesioning technique was validated using histology from *ex vivo* and *in vivo* testing, current and voltage traces from the device, and measurements of spiking activity before and after lesioning. This electrolytic lesioning method avoids disruptive procedures, provides millimeter precision over the extent and submilimeter precision over the location of the injury, and permits electrophysiological recording of single-unit activity from the remaining neuronal population after lesioning. This technique can be used in many areas of cortex, in several species, and theoretically with any multielectrode probe. The low-cost, external lesioning device can also easily be adopted into an existing electrophysiology recording setup. This technique is expected to enable future causal investigations of the recorded neuronal population's role in neuronal circuit function, while simultaneously providing new insight into local reorganization after neuron loss.

Introduction

Neuroelectrophysiology–using electrodes to record the electrical signals generated by neurons–has been the defining technique that shifted neuroscience from macroscale anatomy and loss-of-function studies down to the microscale activity of individual neurons and synapses in a given region of interest ***Sporns*** (***2016***). Prior to the last few decades, electrophysiology was limited to simultaneous recordings of at most five neurons with small numbers of electrodes (typically one, two, or four) ***McNaughton et al.*** (***1983***). The development of neuroelectrophysiology recording techniques with a large number of electrodes starting in the 1970s ***Wise et al.*** (***1970***); ***Campbell et al.*** (***1990***, 1991); ***Rios et al.*** (***2016***); ***Hong and Lieber*** (***2019***) was a boon to systems neuroscience, enabling simultaneous recording from hundreds of neurons and revealing previously unseen aspects of population coding ***Cunningham and Yu*** (***2014***); ***Kalaska*** (***2019***); ***Shenoy and Kao*** (***2021***). Over the last five years, electrode count has continued to increase, with new probes containing thousands of electrodes ***Jun et al.*** (***2017***); ***Steinmetz et al.*** (***2021***); ***Obaid et al.*** (***2020***); ***Musk*** (***2019***). While experiments and analysis have revealed population activity that correlates strongly with behavioral output ***Yu et al.*** (***2009***); ***Churchland et al.*** (***2012***); ***Sadtler et al.*** (***2014***); ***Golub et al.*** (***2018***); ***Elsayed et al.*** (***2016***); ***Goldman et al.*** (***2019***); ***Gallego et al.*** (***2020***); ***Liu et al.*** (***2020***); ***Rasmussen et al.*** (***2017***), novel tools that both record from and inactivate neurons are required to establish causal connections to behavior ***Vaidya et al.*** (***2019***); ***Shenoy and Kao*** (***2021***); ***Slonina et al.*** (***2022***). Although many inactivation methods exist, to date it has been challenging to find a repeatable, long-term inactivation technique compatible with chronic intracortical neuroelectrophysiology.

Design Considerations and Existing Inactivation Methods

Three main design considerations are required for a technique that successfully combines electrophysiology with inactivation (further detailed in ***Appendix 1***).

1. Stable electrophysiology pre- and post-inactivation: Avoiding physical disruption enables direct comparison of pre-lesion activity with both the acute and chronic stages of injury.
2. Ability to localize and control the size of the inactivation: Precise focal inactivations strike a balance between being large enough to alter performance but small enough to spare sufficient tissue to record local re-organization and recovery.
3. Cross-compatibility: A technique that can be used in many areas of cortex, with any multielectrode probe, and in several species will enable causal investigation across a large variety of contexts. A method that works across-species (especially in large-animals like rhesus macaques) would leverage the existing injury literature, recording technologies, and behavioral assays from rodents to new world monkeys, while also being well-suited for the behavioral sophistication and human homology of macaques ***Higo*** (***2021***).

Neuronal activity can either be temporarily or permanently inactivated, defined as manipulation or termination, respectively ***Vaidya et al.*** (***2019***). For clarity, termination refers to a technique that causes death of neurons, removing them from the circuit. We non-exhaustively review existing manipulation and termination techniques in ***Appendix 2***. However, none of these existing techniques meet all of the above design considerations.

Manipulations enable a causal understanding of the relationship between neuronal activity and behavior by studying adaptation to and from a perturbation ***Slonina et al.*** (***2022***). Existing temporary inactivation methods include intracortical microstimulation, optogenetics, pharmacology, transcranial stimulation, cooling loops, and chemogenetics. Since neurons remain anatomically and physiologically viable, manipulations can be easily repeated, until desensitization occurs.

As termination causes cell death, it can generate stronger causal evidence than a manipulation ***Vaidya et al.*** (***2019***). For example, even though a transient manipulation of neuronal activity may temporarily disrupt behavior, only a sustained manipulation could elicit the system's long-term adaption ***Slonina et al.*** (***2022***). Over the days ***Ferrier and Yeo*** (***1884***) and potentially weeks ***Bundy and Nudo*** (***2019***); ***Zeiler et al.*** (***2015***) following a termination, the surrounding circuitry and broader network may adapt, leading to behavioral recovery and demonstrating that although the terminated region was causally implicated in behavioral control in the moment, the terminated neurons are *not themselves* causally necessary. A sustained manipulation could accomplish a similar effect to a termination at the systems level, up to the point at which the manipulation stopped. However, it can be difficult to create sustained inactivation with existing reversible manipulation methods, limiting their ability to study the brain's natural reorganization over timescales of days to months.

Termination methods overcome the problem of sustained and consistent inactivation from which temporary inactivation techniques suffer. Therefore, they enable a form of causal inference not possible with temporary inactivation methods ***Vaidya et al.*** (***2019***); ***Shenoy and Kao*** (***2021***). Existing termination techniques include mechanical trauma, endovascular occlusion, Rose Bengal mediated photothrombosis, and chemical lesioning.

Electrolytic Lesioning Through A Microelectrode Array

In order to best meet the three design considerations, we created a device to make an electrolytic lesion through the same microelectrode array used to record neuronal activity. The dual use of this microelectrode array achieves the first design constraint of stable electrophysiology pre- and post-inactivation, as it enables recording from the exact same signal source with minimal physical disruption or displacement. Aside from the initial implantation of the array, there are no invasive procedures required, removing virtually all risk of destabilizing the recorded population. A further benefit of this surgery-free procedure is avoiding analgesia and sedation and allowing for an unprecedented, minutes-long turn-around between pre- and post-lesion data collection; the experiment can resume as soon as close observation of the animal is complete, the lesion device is disconnected, and the recording stream is reconnected. The electrolytic lesioning technique is repeatable, because the same multielectrode probe can be used many times to create lesions while maintaining stable electrophysiological recordings. Performing electrolytic lesioning requires passing a specified amount of current through two electrodes (one acting as the anode, the other as the cathode). Selecting which electrodes in the microelectrode array should be the anode and cathode sets the

location of the lesion origin. By using a Utah multielectrode array as in this work, the location of the lesion can be changed at a 400µm resolution set by the electrode spacing, while altering the duration and amount of current passed through two electrodes creates changes in the lesion's spatial extent. Thus, while there is still variation in the precise geometry of damage from each lesion, multielectrode-based lesioning does well to satisfy the second design consideration and is a notable refinement from previous lesioning studies. While this platform was designed for use in rhesus macaques, it could be used in other animals in which multielectrode probes can be implanted, such as other primates, large mammals, and rodents. This technique can also be used in effectively any area of cortex in which a multielectrode probe could be implanted. Therefore, this platform is compatible across many cortical areas, across several species, and theoretically across multielectrode probes, fulfilling the third design consideration. As the lesioning device is a small, low-cost external system that only needs to be connected for the duration of lesioning, it is easy to adopt into existing electrophysiology recording settings. This platform is anticipated to facilitate causal explorations of the relationship between brain and behavior through its unique combination of inactivation and neuroelectrophysiology. Further, it should enable studies of natural reorganization at the neuronal population level.

Results

Electrolytic Lesioning Device and Testing

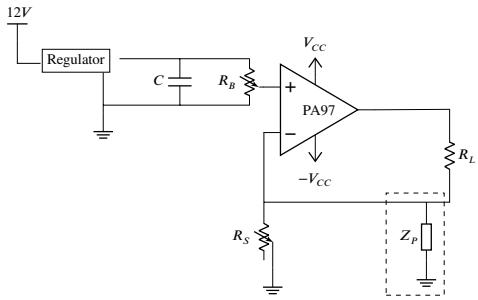

Figure 1. The circuit diagram for the electrolytic lesioning device. An op-amp is used in a negative feedback loop to maintain a constant current through the two electrodes in the brain (R_L). The op-amp was implemented as suggested by its accompanying evaluation kit and supplied components. The system is powered by a 12V power supply, and a boost converter is used to create a V_{CC} and -V_{CC} of 450V and -450V, respectively. The current through R_L can be set by changing the resistance of the potentiometer, R_S. Z_P is a hypothesized physiological parasitic component, which could be either resistive or capacitive (dashed box).

We created a custom current source circuit which allows us to use the same microelectrode array used to record neuronal activity to also create an electrolytic lesion (Fig. 1). The circuit design is based on simple feedback control circuits ***TI*** (***2019***); ***Carter and Brown*** (***2016***); ***TI*** (***2020***) using an operational amplifier ***Mancini and Carter*** (***2009***) to maintain a constant current. While this technique should theoretically work with any multielectrode probe, we performed all proof-of-concept experiments with a Utah microelectrode array (Blackrock Neurotech, Salt Lake City, UT). Lesion size is controlled by the amplitude and duration of the current passed through the two chosen electrodes of the microelectrode array, although the exact extent of damage will vary for each lesion due to anatomical variation. Our circuit supplies the voltage needed to damage cortex while maintaining high precision in the delivered current (precision error not exceeding 10µA). To find a combination of the current amplitude and duration parameters that would create a reasonable lesion size for our use in rhesus macaques, testing was first performed in *ex vivo* sheep and pig brains, and then *in vivo* with anesthetized pigs. Although scientific use of this lesioning device is ultimately intended in rhesus, pilot studies were performed in sheep and pigs in accordance with the guidelines of the National Research Council ***National Research Council (US) Committee on Guidelines for the Use of Animals in Neuroscience and Behavioral Research*** (***2003***); ***National Research Council (US) Committee for the Update of the Guide for the Care and Use of Laboratory Animals*** (***2011***) of replacement, refinement, and reduction (3 R's). Cortex was lesioned using the chosen parameters, after which histology was collected to provide an understanding of lesion quality and extent. Our exploration was not exhaustive and not designed to fully characterize lesion extent as a function of current amplitude and duration; while being mindful of animal use, a key aim was to converge on a parameter set that yielded small, focal lesions suitable for behavioral studies in rhesus macaques with chronic implants. We both sampled the search space of parameter values, current amplitude and duration, and repeated parameter selections for confirmation. Across eleven *ex vivo* and five *in vivo* animals, 61 lesions were performed, including some repeated parameter combinations as biological replicates.

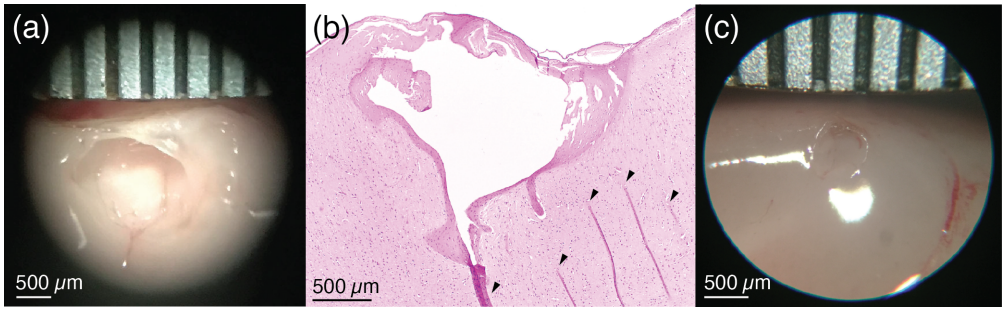

Figure 2. a) *Ex vivo* demonstration of the electrolytic lesion technique in unfixed sheep cerebral cortex using an intracortical Utah microelectrode array. Sustained delivery of 250μA of direct current for 10 minutes between adjacent electrodes (400μm spacing) resulted in a clean spheroidal cavitation in cortex approximately 1.5mm in diameter. Ruler is marked every 500μm. b) Hematoxylin and eosin (H&E) stained slice of the lesion in (a) clearly shows the lesioned region. Arrows indicate tissue fold artifacts that resulted from the histology process, not the lesion. The other dark pink areas surrounding the cavitation in cortex are regions of necrosis. c) A smaller *ex vivo* lesion in unfixed cerebral cortex of another sheep created by decreasing the direct current amplitude and duration to 180μA for one minute. The cavitation has a diameter slightly over 0.5mm.

Ex Vivo Ovine and Porcine Testing

Initial testing was performed in unfixed cortex from sheep and pigs. Prior studies demonstrated that 20 minutes of 400μA direct current resulted in a spherical cavitation in cortex of approximately 2mm in diameter ***Wurtz and Goldberg*** (***1972***). To create a more localized lesion, parameters were reduced substantially to 250μA direct current for 10 minutes, passed through two adjacent electrodes of a Utah array implanted in *ex vivo* sheep cortex. This created a clean spheroidal cavitation in cortex approximately 1.5mm in diameter (Fig. 2a,b), which is consistent with lesion sizes that cause measurable behavioral deficits in the motor system ***Nudo et al.*** (***2003***); ***Wurtz and Goldberg*** (***1972***); ***Glees and Cole*** (***1950***). Although lesions of this size are known to cause significant behavioral deficits, we hypothesized that smaller lesions might lead to deficits that were still noticeable but not detrimental to the animal's overall mobility and mental health, a noted concern in past studies ***Glees and Cole*** (***1950***). Reducing the duration and intensity of the current used to lesion created smaller cavitations in cortex: one minute of 180μA direct current, passed through two adjacent electrodes in *ex vivo* pig cortex, created a smaller spheroidal cavitation of approximately 0.5mm in diameter (Fig. 2c).

In Vivo Porcine Testing

In vivo testing allowed for further parameter refinement in the presence of natural acute inflammatory responses. By further reducing the duration and intensity of the current used to lesion, the extent of the cavitation in the cortex was reduced to the point where there is no longer a cavitation but instead a clear region of damaged parenchyma. One minute of 150μA direct current, passed through two adjacent electrodes in pig cortex resulted in a well-demarcated region of parenchymal damage (Fig. 3a). The region of parenchymal damage appears paler on H&E staining than the adjacent, unaffected parenchyma and was confined to an upside-down conical region, which was 3.5mm wide at the cortical surface and extended approximately 2mm deep. Within this region (seen magnified in Fig. 3b), there was widespread coagulative necrosis, parenchymal rarefaction, and perivascular microhemorrhage. Acidophilic neuronal necrosis was identified along the marginal boundaries of the region of coagulative necrosis. Adjacent neural parenchyma was unaffected (representative selection shown in Fig. 3c), demonstrating the relatively precise boundary of damage caused by the electrolytic lesion. The physical damage visible as tears in the tissue (white) near the surface of this damaged cone of tissue may be due to withdrawal of the microelectrode array from cortex after testing. In control tests where a microelectrode array was inserted and removed but no current was used to create a lesion (Table S1 and Table S2), regional coagulative necrosis was not present, and cortical damage was confined to mild subcortical and/or perivascular microhemmorage and scattered individual neuronal necrosis, typically in regions adjacent to microvascular hemorrhage. This emphasizes that electrolytic lesioning, not array insertion alone, leads to coagulative necrosis. This testing was performed across many regions of porcine cortex, demonstrating that the electrolytic lesioning technique functions in any area of cortex in which a multielectrode probe can be implanted.

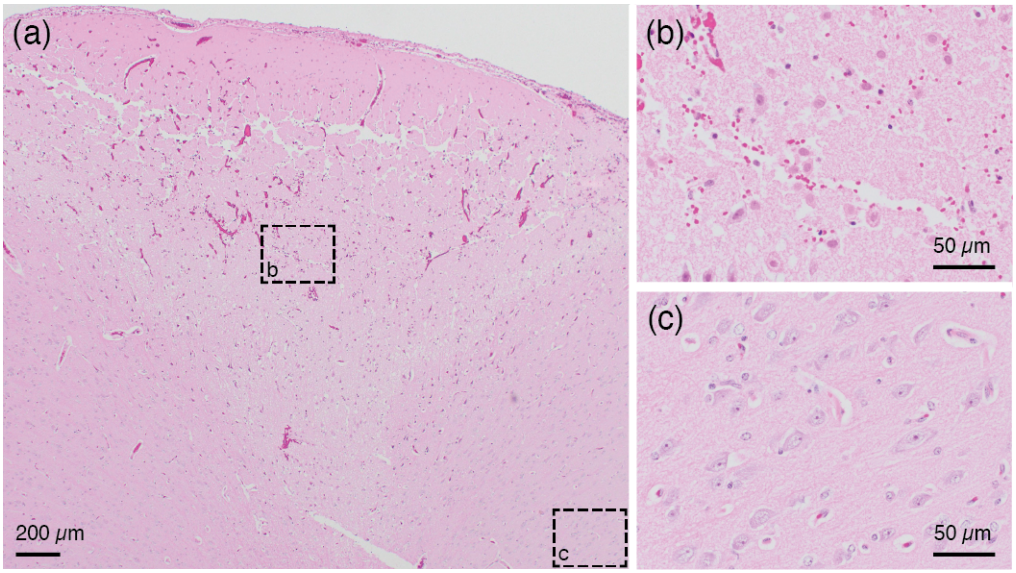

Figure 3. a) H&E stained slice from an *in vivo* demonstration of the lesioning technique in pig cerebral cortex. 150μA direct current passed through two adjacent electrodes (400μm spacing) for one minute resulted in a conical region of damaged parenchyma. The top of the conical region shows a line of damage which may be caused by physical removal of the microelectrode array after testing. Anatomically observed alterations are clearly demarcated, emphasizing the fine localization of the lesioning method. b) Region of intermixed necrotic and histologically normal neurons within the conical zone of damage is visible in a close-up of the slice from (a). Necrotic neurons have shrunken cell bodies. The microelectrode array is expected to continue recording from remaining healthy neurons after performing a lesion. c) Region of viable neurons outside the conical region of damage is visible in a close-up of the slice from (a). This shows the precise spread of the method, with intact, viable tissue present just outside the lesioned area.

In Vivo Use in Rhesus Macaques

After this validation and refinement, one proof-of-concept lesion was performed in an *in vivo* sedated rhesus macaque (Monkey F) in order to validate the safety of the procedure. This technique has since been used successfully in experimental settings with two other awake-behaving rhesus macaques (Monkeys H & U), for a total of fourteen lesions using thirteen unique electrode pairs.

Current and Voltage Output

In all of the fourteen lesions across two awake-behaving rhesus macaques, the current source worked as expected, providing a constant current throughout the duration of the procedure. Fluctuations in current amplitude were likely due to the 10μA precision of the multimeter used to read out the current (e.g., the readout would sometimes switch between 150μA and 160μA). The voltage across the microelectrode array also generally behaved as expected (Fig. 4). Upon turning on the lesioning device, the voltage initially increased sharply, sometimes exceeding the slew rate of the voltmeter (seen as a discontinuity in the traces in Fig. 4). Due to the limited resolution of the voltmeter, the voltages were unknown between 0.13 and 0.33s but could not have exceeded 900V based on V_{CC} and -V_{CC}. After this peak, the voltage predominantly levels off.

Duration of the applied current is controlled by a switch that cuts the power to the boost converter. However, after the power to the boost converter is removed, the current supplied by the circuit briefly persists — likely due to residual energy present in the capacitors of the boost converter downstream of the switch. In the lesions for which this data was collected, the current persisted at the calibrated intensity for between 2.5 and 4 seconds.

Before performing a lesion, the amount of current to be output by was calibrated using a 50Ω resistor in place of the implanted microelectrode array and altering the resistance level of the external potentiometer. Even when calibrated to generate 150μA, the actual current output when lesioning differed slightly (10 to 20μA above or below the set value). In nine out of the fourteen lesions performed in two awake rhesus macaques (thirteen of which had this voltage data collected), the current value was higher than what was calibrated. We hypothesize that this is due to a parasitic parallel resistance to ground through the animal itself (see dashed box in Fig. 1). To have created

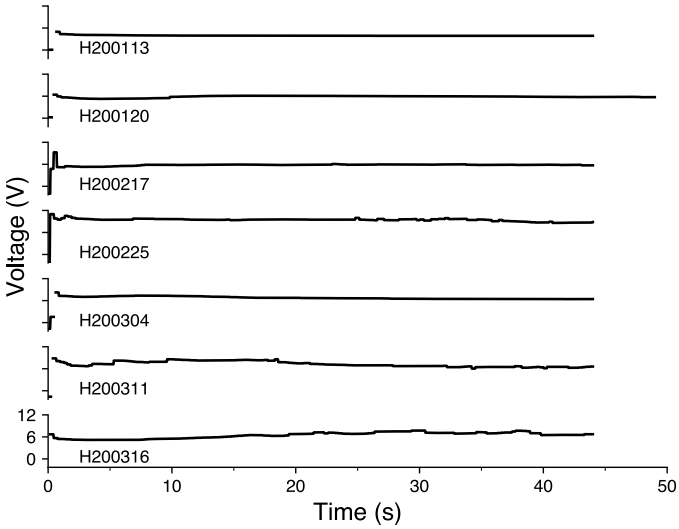

Figure 4. Voltage traces from seven representative lesions in an awake-behaving rhesus macaque (Monkey H). Lesions are shown in chronological order and are labeled with an experimental ID in the form SYYMMDD, where S indicates the animal, followed by the date. Discontinuity at the beginning of the traces indicates transient voltages that were too rapid to be captured by the voltmeter, lasting between 0.13 and 0.33s. Traces only capture the voltage while the lesioning device was turned on (45 seconds for most lesions and 50 seconds for lesion H200120).

the 10 to 20μA increase in current above the set value, this parasitic parallel resistance would have been between 1.2MΩ and 0.6MΩ, respectively, which is in the range of the expected resistance when the body is in dry contact with the environment ***Fish and Geddes*** (***2009***). In the three lesions where the current value was 10 to 20μA lower than what was calibrated, there may have been some parasitic capacitance present. As these parasitic resistances and capacitances arise only when the animal is part of the experimental setup, and they change across sessions, they cannot readily be calculated and accounted for *a priori*. These parasitics appear small enough not to significantly impact the desired lesion characteristics.

Recording Quality

One advantage of microelectrode arrays is their ability to record from a stable population of cortical neurons over months ***Vaidya et al.*** (***2014***); ***Dickey et al.*** (***2009***); ***Fraser and Schwartz*** (***2012***); ***Ganguly and Carmena*** (***2009***). While the exact neurons captured from the local population vary day-to-day, they largely remain the same, which enables researchers to sample the activity of a consistent neuronal population over time.

Comparisons of the recorded action potential waveforms before and after multiple lesions revealed that microelectrode arrays were able to continue recording stable neuronal activity in awake-behaving rhesus (e.g., lesion six, performed in Monkey H, and lesion 11, performed in Monkey U; Fig. 5a). Surprisingly, even the lesion electrodes themselves continued to record reliably, suggesting that the modest electrolytic lesion intensity used is not prohibitively destructive to an electrode's recording ability. Given the majority of waveforms appear unaltered (Fig. 5a), it seems unlikely that any acute damage response globally shifted the array away from the recorded neuron population.

After an electrolytic lesion, a small percentage of the recorded waveforms appeared to change significantly, which may be a result of neuron damage or death, or may be an adaptive neuronal circuit response to lesioning. Since the lesion experiments performed in Monkeys H and U were not terminal studies, definitive histological evidence of neuron loss could not be acquired. Therefore, as a proxy for neuron loss, the relative change in the daily turnover of recorded neurons was assessed (Fig. 5b; see Methods for details). To minimize any potential ambiguity, the analysis was restricted to four consecutive lesions in Monkey U (lesions 11-14) that were spaced weeks apart, allowing ample time for stable recovery and for each lesion to be treated as an independent sample —

∗ HL6

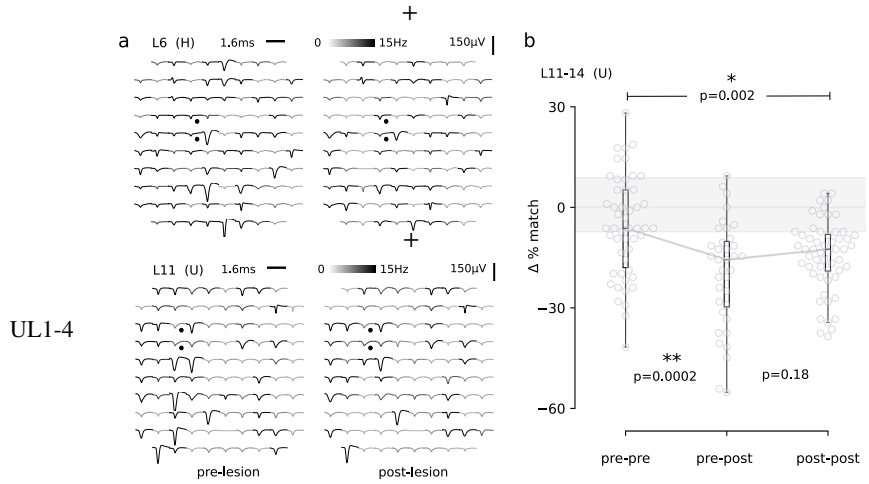

Figure 5. a) A representative comparison of recorded action potential waveforms, before and after the sixth and eleventh lesions (*top*, Monkey H; *bottom*, Monkey U). The location of the lesion electrodes on the arrays' spatial layout are marked by black dots. Good quality signal was observed in the recording sessions immediately before and after lesioning (*left, right*). An action potential detection rate was determined from periods of task engagement (gray-scale shading, capped at 15Hz for visualization). b) As a proxy for neuron loss, a relative turnover in daily recorded neurons was determined by pairwise comparisons of action potential waveforms within three groups: pre-lesion days (pre-pre), pre-lesion versus post-lesion days (pre-post; up to three days post-lesion), and post-lesion days (post-post; four to nine days after a lesion). An inter-quartile range is shaded in grey for the set of 10 consecutive days leading up to lesion 11, the first in Monkey U. The median from this healthy control group was subtracted from all other pairwise comparisons to directly quantify a change in turnover. This pre-lesion group was then combined with the other pre-pre comparisons and tested against the pre-post and post-post groups. The change in the percentage of matching neurons dropped significantly after a lesion (Median test; * < 0.003, ** < 0.0003, corresponding to corrected significance levels of 0.01 and 0.001 for the three comparisons). Note, lesions 11-14 in Monkey U were well-spaced out over three months and considered as independent samples.

recovery time courses in Monkey H were longer and less cleanly separated.

A healthy control set of the ten days preceding the first lesion (L11) was used to draw pairwise recordings and calculate the median and quartile values (25th and 75th percentiles Fig. 5b). For each lesion, pairwise daily recording sessions were drawn from a set of thirteen contiguous recording days (four pre-lesion days and nine post-lesion days). The pre-post group included up to three days following a lesion, while the post group considered post-lesion days four to nine and was intended to reflect a late post period (not necessarily a complete recovery of brain and behavior). All pairwise comparisons were separated by no more than four days to keep turnover rates stable ***Gallego et al.*** (***2020***). Action potential waveform data from lesions 11-14 and the pre-lesion control set were pooled and grouped into the same pre-pre, post-pre, and post-post categories for a summary comparison (Fig. 5b). Following lesions, the percentage of matching neurons in the pre-post group dropped below the expected percentage of matching neurons among pre-lesion days, appearing to trend back toward comparable levels in the post-lesion group despite still being significantly decreased. This drop in the percentage of matching neurons after lesioning suggests, despite us not having access to histology to confirm, that the lesions terminated neurons.

Discussion

In this report, we demonstrated a novel method for electrolytic lesioning through a microelectrode array that is compatible with electrophysiological recording of neuronal activity pre- and post-lesion. To achieve this, a custom current source was built that would ensure stable current delivery throughout the lesion, for repeated lesions, as well as across different electrode types and animals. This degree of control represents a significant refinement of lesion studies in systems neuroscience research. This model was tested *ex vivo* with porcine and ovine brains and *in vivo* with porcine brains. Altering the amount and duration of the current changed the size of the lesion, as evidenced by the histology. Selection of two adjacent lesion electrodes allows for spatial localization under the $16mm^2$ array. Following these preliminary tests, one lesion was performed in a sedated rhesus macaque to verify the safety of the procedure and obtain primate histology, and fourteen lesions were performed between two

awake rhesus macaques. Readouts from the lesioning device itself (both current and voltage) and electrophysiology from the microelectrode array verify that the device delivers the desired power and does not damage the array's recording ability. We believe that this electrolytic lesioning technique will improve understanding of the motor system by coupling lesioning (an established termination technique) with the detailed spatiotemporal measurements of intracortical electrophysiology ***Shenoy and Kao*** (***2021***); ***Vaidya et al.*** (***2019***).

Although it shares elements with other widely used techniques, performing electrolytic lesioning through a microelectrode array is not a common inactivation technique. For example, injecting current into the brain through microelectrodes is commonly done in intracortical microstimulation ***Weiss et al.*** (***2019***). However, typical current values for microstimulation are around three times smaller than for lesioning, pulse durations are on the order of tens of microseconds, and the pulses by design do not lead to cell death or materially affect the electrodes. Similarly, passing current through microelectrodes to mark their location in cortex is a well-established method for tracking the location of electrodes at the end of an animal study. When histology is eventually performed, the lesion is used to find the anatomical location where electrophysiology was conducted, and it is compatible with single or multi-channel electrodes ***Chen et al.*** (***2009***). However, the intent is different, as electrolytic lesions for marking are not generally used as an inactivation technique. Electrolytic lesioning for inactivation was historically done through a single barrel electrode as the anode and without any post-lesion electrophysiology recordings ***Wurtz and Goldberg*** (***1972***). Therefore, the electrolytic lesioning method for inactivation presented here both is a refinement in precision and is unique in its compatibility with electrophysiology.

Electrolytic lesioning leads to cell death through heat ***Nikfarjam et al.*** (***2005***), electroporation ***Batista Napotnik et al.*** (***2021***), and local changes in pH ***Nikfarjam et al.*** (***2005***). Demonstration of actual neuronal loss in a primate injury model must work within the guidelines of ethical animal research. Therefore, we have triangulated evidence from three distinct sources that indicate the electrolytic lesioning device reliably delivered current that caused tissue damage and neuron death (termination): *ex vivo* and *in vivo* histology (Figs. 2, 3), lesion device readouts (Fig. 4), and relative changes in the turnover rate of recorded neurons *in vivo* (Fig. 5). Despite observing temporary increases in the day-to-day turnover after lesioning (decrease in the percent of matching neurons), it should be noted that this is likely an underestimate as significant neuronal loss may also be occurring nearby, just outside of the electrodes' recording volume and thus evading detection. The histology presented here indicates regions of partially damaged tissue in which dead neurons are randomly interspersed and whose termination will inevitably vary depending on their proximity to the nearest electrode. It is evident in our recordings that many of the array's electrodes are recording smaller inseparable waveforms corresponding to multiple neurons located between between 50μm and 140μm from the electrode tip before the lesion ***Buzsáki*** (***2004***); ***Gerstein and Clark*** (***1964***). Even if the closest, more cleanly separated neurons were terminated by the lesion, the recorded signal would still be comprised of the remaining, surviving neurons in that vicinity. These neurons may also become more active after injury resulting in seemingly similar firing rates. This was likely the case for lesion six (Monkey H; Fig. 5a top) and lesion 11 (Monkey U; Fig. 5a bottom), where the average waveforms on the two lesion electrodes themselves appear similar with only slight differences in amplitude. These small shifts will affect the cluster shape when spike-sorting, but are unlikely to be classified as a distinct neuron cluster. Therefore, turnover rate estimates from our *in vivo* lesions in non-human primates (Fig. 5) are likely underestimating the true extent of neuronal loss. However, there is the potential to overestimate loss as well, given it is impossible to disambiguate between neurons that were silenced but surviving versus truly terminated. Under the constraints, we note that these sources of error may be somewhat counterbalanced.

While we have thoroughly tested this electrolytic lesioning device to ensure proper function, we emphasize that this is an initial design of the device and a preliminary examination of lesion parameters. We have only begun to explore the full potential for electrolytic lesioning through a microelectrode array, in both its technical implementation and its future use in systems neuroscience. This technique was tested across three species, settling on a combination of current amplitude and duration that seemed reasonable for experiments in awake-behaving rhesus macaques. Thorough testing had to be balanced with care and respect for appropriate animal use in accordance with the 3 R's of the guidelines of the National Research Council ***National Research Council (US) Committee on Guidelines for the Use of Animals in Neuroscience and Behavioral Research*** (***2003***); ***National Research Council (US) Committee for the Update of the Guide for the Care and Use of Laboratory Animals*** (***2011***). Future alterations could be made to the design of the lesioning device itself to optimize lesioning through this platform. For

example, electronic control of current delivery for lesioning could be refined through the use of digital switching and a resistor shunt to handle any leakage current. Even with such automation, it would be prudent to maintain a physical switch to prevent extremely long periods of current delivery in the case of a malfunction. A circuit revision with these refinements has been designed and validated, but it has not yet been tested in animals out of aforementioned respect for animal use.

Further exploration into the amplitude and duration parameters of the current used to lesion could lead to markedly different impact on brain tissue. Although these lesions were created with DC current, a variety of current patterns could be used to create a lesion. Catheter ablation of the heart used to be performed with DC current ***Scheinman*** (***1982***); ***Gallagher et al.*** (***1982***). Now, the standard of care is using a radiofrequency (350-500 kHz) alternating current ***Shivkumar*** (***2019***); ***Morady*** (***1999***). Similarly, some have explored using radiofrequency (55kHz) alternating current to create lesions to mark the location of acute electrophysiological recordings ***Brozoski et al.*** (***2006***). It is likely that alternating current or more complex current patterns would lead to different spatial distributions of electrolytic lesions. The PA97 op-amp used in this lesioning device has a slew rate of $8\mathrm{V}/\mu\mathrm{s}$, and can support AC frequencies in the tens to hundreds of kHz range for the lesioning voltages seen here. At the same time, AC currents would likely introduce new reactive parasitics, potentially along the electrode wire bundle or at interconnects, and should be evaluated carefully.

Different selection of electrodes within the microelectrode array could also lead to different lesion characteristics. We chose to lesion with adjacent electrodes only, in order to create the most focused lesion. In theory, larger ablations are possible by supplying larger currents or performing a lesion over non-adjacent electrodes, which can span as much as 5.6mm for electrodes on the opposite corners of the 4mm x 4mm Utah array.

Electrode shape could also be used to create different lesions. In deep brain stimulation treatment for Parkinson's disease, new electrodes were designed to directionally focus the stimulation ***Steigerwald et al.*** (***2019***). Similar design could be used in creating intracortical electrodes for elctrophysiology and electrolytic lesioning.

The electrolytic lesioning method presented here enables small, permanent inactivation volumes while maintaining reliable neuroelectrophysiological recordings. Selection of the electrical current pattern, amplitude, and duration, as well as the specific lesion electrodes' shape and location, offers many different combinations for complementary investigations into the causal role of cortical activity.

Materials and Methods

Electrolytic Lesioning Device Design

In order to control lesion size, a current source is required to stabilize the output, due to changes in local tissue resistivity and the design of intracortical electrodes. Single unit electrodes are generally coated with some type of dielectric material to maintain a low surface area of exposed metal, yielding a high impedance. This high impedance enables the detection of the weak currents (order tens of nA) associated with single neuron action potentials with voltages on the scale of tens to hundreds of microvolts ***Carter and Shieh*** (***2015***). The shafts of the Utah electrode array are insulated with parylene-C (Blackrock Neurotech, Salt Lake City, UT). A small area at the tip of each electrode remains uncoated, through which the ionic current from nearby neurons can be measured. During electrolytic lesioning, applied voltages can be large enough to etch off the dielectric coating from the shaft of the two electrodes used to lesion. As this coating is etched, the impedance of those electrodes falls. Using a constant voltage source to lesion could deliver an inappropriately large amount of current into the brain once the dielectric coating was etched off and impedance reduced, resulting in uncontrolled tissue damage. A constant current source is robust to this changing impedance, maintaining the desired electrical current.

Single unit electrodes are commonly manufactured to have an impedance on the order of 100kΩ to 1MΩ ***Maynard et al.*** (***1997***). In past electrolytic lesioning studies, the currents used to create lesions with corresponding behavioral deficits were on the order of 100µA ***Glees and Cole*** (***1950***); ***Wurtz and Goldberg*** (***1972***). Therefore, in order to supply this current in the face of the high impedance dielectric coating associated with single unit electrodes, high tens to low hundreds of volts are needed, depending on the lesioning parameters chosen. Even though commercial devices exist for electrolytic lesioning (e.g., Ugo Basile, Gemonio, IT), the power supplied may not be sufficient to recreate some current amplitudes used to lesion in literature ***Wurtz and Goldberg*** (***1972***) and generally only support DC waveforms.

We designed and built a custom current source circuit (Fig. 1) that supplies this voltage while maintaining precision in the delivered current (precision error not exceeding 10µA). The circuit features a commercial power operational amplifier, PA97 (Apex Microtechnology, Tucson, AZ), in a negative feedback loop ***DePaola* (*2020*)**, implemented in accordance with the corresponding evaluation kit, EK28 (Apex Microtechnology, Tucson, AZ). Power is provided through a 12V external power supply, and a boost converter is used to create a V_{CC} and -V_{CC} of 450V and -450V, respectively. These are both low-cost, off-the-shelf, readily-available discrete circuits. The amplitude of the current supplied through between the cathode and anode to the brain (shown as the load, R_L) is tuned through altering the value of a variable potentiometer (R_S). The voltage supplied to the op-amp can also be altered by altering the bias resistance with the potentiometer, R_B. The total cost of the parts needed is approximately three hundred US dollars, making it an affordable addition to a neuroelectrophysiology recording setup.

Experimental Setup

The lesioning device is built as a contained box, to which the power supply, measurement devices, and microelectrode array are externally connected (Fig. S1). An external switch on the lesioning device controls the power to the boost converter. This is the switch that is manually turned on and off to control the duration of current delivery for lesioning. The lesioning device is connected to two electrodes from the intracortically implanted microelectrode array (R_L). All lesioning was performed using Utah electrode arrays with the same specifications (Blackrock Neurotech, Salt Lake City, UT). The arrays are 4mmx4mm, with 96 channels. Electrode shafts are made of silicon (Si) with a metallic outer layer (platinum or platinum-iridium), and coated with parylene-C. Electrodes are 1mm in length and have a 400µm inter-electrode spacing. The array is connected to the lesioning device with the array's external CerePort (Blackrock Neurotech, Salt Lake City, UT) and a CerePort breakout adaptor that connects to specific electrodes from the array. A Fluke 179 True-RMS Digital Multimeter (Fluke Corporation, Everett, WA) is used as an ammeter in series before R_L to measure the current passing through R_L (the desired output). A voltmeter spans R_L to measure the voltage delivered. The variable potentiometer R_S is tuned by a dial on the outside of the lesioning device, allowing quick and easy calibration of the amplitude of the current.

All animal procedures and protocols were approved by the Stanford University Institutional Animal Care and Use Committee (IACUC).

Ex Vivo Ovine and Porcine Testing

Initial testing of lesion parameters was performed *ex vivo* in three sheep and eight pig brains (Table S1). These un-fixed brains were from animals that were euthanized earlier that day for unrelated research and/or teaching efforts, in line with the reduction principle of animal research ***National Research Council (US) Committee on Guidelines for the Use of Animals in Neuroscience and Behavioral Research* (*2003*)**; ***National Research Council (US) Committee for the Update of the Guide for the Care and Use of Laboratory Animals* (*2011*)**. As these brains were from unrelated research efforts, we were not given the sex or exact age of the animals. The brain was kept moist with saline throughout the procedure. A Utah array was implanted with a pneumatic insterter (Blackrock Neurotech, Salt Lake City, UT) into suitably large and flat gyri. The lesioning device was then connected to the microelectrode array and used to create a lesion. The location of the array implantation was marked using a histology pen or ink injection and detailed for the research record. The brains were then fixed, sliced, and prepared with hematoxylin and eosin (H&E) staining.

In Vivo Anesthetized Porcine Testing

We next sought to determine how lesion size might be altered *in vivo*, where blood flow, microhemorrhage, and the body's acute inflammatory responses could affect the lesion extent and intensity over time. Testing was performed on five anesthetized pigs, to evaluate the *ex vivo* current amplitude and duration parameters in the context of inflammatory responses (Table S2).

Each pig was sedated and then intubated, ventilated, and placed on inhaled isolflurane. Once under anesthesia and the airway was confirmed, the head was secured in preparation for the procedure. After preparing and cleaning the surgical area, a midline skin incision was made and all skin, muscle, aponeurosis, and periosteum were retracted to expose the skull. Most of the dorsal surface of the skull was exposed along with some of the lateral margins to visualize the anatomy. A single, large craniectomy, exposing most of the superior surface of the dura, was made using a high speed bone drill (ANSPACH, DePuy Synthes, Raynham, MA). Once the craniectomy was at the

desired size and location, the dura was washed with saline and hemisphere-wide dural flaps were made to expose the brain. Once exposed, the brain was covered with gauze and kept moist with saline throughout the procedure.

The implantation and lesion procedures were completed in the same manner as in the *ex vivo* testing. After lesioning, the array was either removed by hand and placed at a new cortical location for further testing or, if the last lesion of the procedure, was left in place for two to three hours before euthanizing the animal to even better mimic the post-lesion inflammatory response. Therefore, histology for all lesions included the physiological response to lesioning after at least two to three hours, and some lesions also retained the array in place as a foreign body during this post-lesion time frame. After the final lesioning was complete and sufficient time had elapsed for lesions to appear histologically, the pig was euthanized via IV injection of beauthanasia solution (100mg/kg, IV). The brain was then fixed, and slices were prepared with H&E staining.

In Vivo Lesions in Rhesus Macaque

Electrolytic lesioning is not painful as there are no direct pain receptors in the central nervous system ***Hall and Hall*** (***2021***). Based on this, and a lack of physiological signs of pain from the anaesthetized pig studies, a lesion was performed on a sedated rhesus macaque (Monkey F; 16 year-old adult, male rhesus macaque) in order to further verify safety before use in awake-behaving rhesus. Again, no physiological signs of stress or complications were observed, increasing confidence for lesions in awake animals. Subsequently, lesions were safely performed in two other rhesus (Monkeys H and U; 14 and 11 years-old, respectively, adult, male rhesus macaques) while awake and seated in a primate chair, without the animals exhibiting any behavioral signs of stress or pain. Across these two animals, fourteen lesions were performed using thirteen unique electrode pairs, demonstrating that the same microelectrode array can be used for several lesions and even the same electrode pair can be used as the anode and cathode for multiple lesions. The Utah array chronically implanted in the monkey's cortex is connected to the lesioning device via its CerePort (the same one used for recording the neuronal signals from the microelectrode array). The lesioning device is then turned on for a fixed duration, delivering the desired current. The animal is continuously monitored during the procedure for any signs of discomfort. After lesioning is complete and the recording cables are re-connected to the CerePort, the monkey is immediately ready to resume electrophysiological recordings and participate in a wide variety of head-fixed or freely moving behavioral paradigms. Although lesioning itself is painless, the technique is intended to cause a temporary functional impairment. In light of this, monitoring of animal behavior post-procedure is conducted by research staff in coordination with veterinary staff to ensure health, safety, and psychological well-being.

Neuronal Recordings and Processing

Neuronal data was collected at 30kHz from primary motor cortex of Monkeys H and U using a Utah array (described above), captured using a Cerebus system (Blackrock Neurotech, Salt Lake City, UT), then high-pass filtered offline with a fourth order, zero-phase Butterworth filter using a 250 Hz cutoff frequency. Action potentials were identified by thresholding the filtered membrane potential at $-4\times$ the root mean square voltage measured over the first minute of the recording session. Data snippets for comparing electrophysiology pre- and post-lesion were generated by taking the preceding 16 sampled data points (0.53ms), and proceeding 32 sampled points (1.07ms) around these identified threshold crossings. Waveforms whose peak-to-trough amplitude exceeded 300µV are atypical of extracellular recordings from cortical neurons and were excluded ***Chestek et al.*** (***2011***). Waveform width was calculated as the difference between the two prominent peaks in the temporal derivative of the extracellular potential. Unphysiological waveforms whose widths were longer than 1ms were also excluded ***Bean*** (***2007***). The remaining identified action potential waveforms were then averaged for each electrode and event rates were determined as the number of spikes on a given electrode divided by the duration of the recording session (excluding brief periods of inactivity before the start of the session).

As a putative indication of neuronal loss, the relative change in neuron turnover was measured between daily recording sessions (each pair separated by at most three days). For a given electrode, identified action potentials from the first day's recording session were spike-sorted, then the same waveforms were pooled with the second day's waveforms and sorted again. Sorting was performed by projecting a given set of waveforms onto their top two principal components and running hierarchical clustering on these scatter points using the fclusterdata function from SciPy's cluster.hierarchy package (SciPy version 1.6.3) ***Virtanen et al.*** (***2020***). The distance threshold for cluster

identification was set as 4.5 (arbitrary units) as it appeared to represent the data well and generated results consistent with turnover rates observed in healthy primate cortex ***Gallego et al.*** (***2020***). Although a range of threshold values would likely be valid, the precise value is not a concern here since we are seeking to identify relative changes in neuron turnover. If fewer clusters were identified when waveforms from both days were combined (neurons lost) or more clusters were identified (new neurons detected), then that electrode was designated as altered by the lesion. It is assumed that previously undetected neurons largely reflect compensation to the loss of other nearby neurons, which were not recorded by the array or were present in the background multi-unit activity. The fact that the majority of waveforms on the array are consistently the same alleviates the concern that simple shifts in the relative position of the tissue explains the altered waveforms. Otherwise, electrodes with matching waveforms were deemed unaltered and presented as a percentage of the array's total 96 electrodes for that pair of days (% match). While inter-spike interval statistics are commonly used as a feature to help identify distinct neurons in healthy animals, they are likely not appropriate here, since surviving neurons may drastically alter their activity after injury.

These pairwise clustering comparisons were then split up into three groups: pre-lesion versus pre-lesion days (pre-pre), pre-lesion versus post-lesion days (pre-post), and post-lesion version post-lesion days (post-post). Although a set of thirteen consecutive days was analyzed for a given lesion (four pre- and nine post-), only recording session pairs that were separated by four-days or fewer were analyzed in order to minimize the potential confound of increased turnover resulting from more than a few days of separation ***Gallego et al.*** (***2020***). Comparisons were then made between the pre-lesion period, an acute injury period (up to three days following a lesion), and a late recovery period (days four to nine following a lesion). The Median test was used to test the null hypothesis that lesioning had no effect on recorded turnover with 99% and 99.9% confidence intervals Bonferroni corrected for the three statistical comparisons made between groups ($\alpha/3$, significant if $p < 0.003$, * or $p < 0.0003$, **). The ten pre-lesion days leading up to the first lesion in Monkey U were also compared to establish a median and inter-quartile range as a healthy control. This median value, 72%, was subtracted from the percentage change in each group to determine a relative change in the matching waveforms between days after injury (Δ% match).

Acknowledgements

We thank S. Baker for veterinary support, and M. Truong and K. Chin for administrative support. The members of the Brain Interfacing Laboratory are Kristina Lebedev, Michelle S. Wechsler, Mackenzie J. Risch, Stephen I. Ryu, Alissa S. Ling, Michael P. Silvernagel. M. S. Wechsler and M. J. Risch were responsible for animal care, surgical support, and guiding behavioral training. S. I. Ryu was responsible for nonhuman primate array implantation. Alissa S. Ling and Michael P. Silvernagel assisted in animal care and porcine surgeries.

Additional Information

Competing Interests

The authors declare that no competing interests exist.

Funding

Research reported in this publication was supported by the Stanford University Wu Tsai Neurosciences Institute, an American Heart Association Predoctoral Fellowship - 828653 to IEB, a NSF GRFP DGE - 1656518 to IEB, and a Stanford School of Medicine's Dean's Posdoctoral Fellowship to SEC.

Author Contributions

P.N. conceived of, designed, and constructed the lesioning circuit (conceptualization, methodology, resources). P.N., S.C., and I.B. validated the circuit design (methodology, validation) and I.B. created the schematic (visualization). S.C. and P.N. were responsible for *ex vivo* testing (investigation). I.B., S.C., and P.N. were responsible for *in vivo* porcine testing (investigation). K.C. performed histology on samples from both *ex vivo* and *in vivo* testing (data curation), and I.B. annotated the figures (visualization). S.C. and I.B. were responsible for non-human primate neuroelectrophysiology experiments and lesioning (investigation). I.B. analyzed the voltage data (formal analysis, visualization). S.C. performed the turnover analysis (formal analysis, visualization). I.B. wrote the original draft (writing - original draft preparation). I.B., S.C., P.N., and K.C. reviewed and edited the manuscript (writing - review & editing). P.N. was involved in all aspects of the project (conceptualization, supervision, funding acquisition).

Data Availability

All data shown are available within the figures and tables.

References

Non-inverting op amp with non-inverting positive reference voltage circuit. Texas Instruments Incorporated; 2019.

AN-31 amplifier circuit collection. Texas Instruments Incorporated; 2020.

Batista Napotnik T, Polajžer T, Miklavčič D. Cell death due to electroporation – A review. Bioelectrochemistry. 2021 10; 141:107871. doi: 10.1016/j.bioelechem.2021.107871.

Bean BP. The action potential in mammalian central neurons. Nature Reviews Neuroscience. 2007 6; 8(6). doi: 10.1038/nrn2148.

Berndt A, Lee SY, Ramakrishnan C, Deisseroth K. Structure-guided transformation of channelrhodopsin into a light-activated chloride channel. Science. 2014 4; 344(6182):420–424. doi: 10.1126/science.1252367.

Brozoski TJ, Caspary DM, Bauer CA. Marking multi-channel silicon-substrate electrode recording sites using radiofrequency lesions. Journal of Neuroscience Methods. 2006 1; 150(2). doi: 10.1016/j.jneumeth.2005.06.012.

Bundy DT, Nudo RJ. Preclinical Studies of Neuroplasticity Following Experimental Brain Injury. Stroke. 2019 9; 50(9):2626–2633. doi: 10.1161/STROKEAHA.119.023550.

Buzsáki G. Large-scale recording of neuronal ensembles. Nature Neuroscience. 2004 5; 7(5):446–451. doi: 10.1038/nn1233.

Campbell PK, Jones KE, Normann RA. A 100 electrode intracortical array: Structural variability. In: *Biomedical Sciences Instrumentation*, vol. 26 Publ by ISA Services Inc; 1990. p. 161–165.

Campbell PK, Jones KE, Huber RJ, Horch KW, Normann RA. A silicon-based, three-dimensional neural interface: manufacturing processes for an intracortical electrode array. IEEE Transactions on Biomedical Engineering. 1991; 38(8). doi: 10.1109/10.83588.

Carmichael ST. Rodent models of focal stroke: Size, mechanism, and purpose. NeuroRX. 2005 7; 2(3). doi: 10.1602/neurorx.2.3.396.

Carter B, Brown TR. Handbook of Operational Amplifier Applications. Texas Instruments Incorporated; 2016.

Carter M, Shieh J. Electrophysiology. In: *Guide to Research Techniques in Neuroscience* Elsevier; 2015.p. 89–115. doi: 10.1016/B978-0-12-800511-8.00004-6.

Chen X, Zirnsak M, Vega GM, Govil E, Lomber SG, Moore T. Parietal Cortex Regulates Visual Salience and Salience-Driven Behavior. Neuron. 2020 4; 106(1):177–187. doi: 10.1016/j.neuron.2020.01.016.

Chen YY, Lai HY, Lin SH, Cho CW, Chao WH, Liao CH, Tsang S, Chen YF, Lin SY. Design and fabrication of a polyimide-based microelectrode array: Application in neural recording and repeatable electrolytic lesion in rat brain. Journal of Neuroscience Methods. 2009 8; 182(1). doi: 10.1016/j.jneumeth.2009.05.010.

Chestek CA, Gilja V, Nuyujukian P, Foster JD, Fan JM, Kaufman MT, Churchland MM, Rivera-Alvidrez Z, Cunningham JP, Ryu SI, Shenoy KV. Long-term stability of neural prosthetic control signals from silicon cortical arrays in rhesus macaque motor cortex. Journal of Neural Engineering. 2011; 8(4). doi: 10.1088/1741-2560/8/4/045005.

Churchland MM, Shenoy KV. Delay of movement caused by disruption of cortical preparatory activity. J Neurophysiol. 2007; 97:348–359. doi: 10.1152/jn.00808.2006.

Churchland MM, Cunningham JP, Kaufman MT, Foster JD, Nuyujukian P, Ryu SI, Shenoy KV, Shenoy KV. Neural population dynamics during reaching. Nature. 2012; 487(7405). doi: 10.1038/nature11129.

Clark TA, Sullender C, Kazmi SM, Speetles BL, Williamson MR, Palmberg DM, Dunn AK, Jones TA. Artery targeted photothrombosis widens the vascular penumbra, instigates peri-infarct neovascularization and models forelimb impairments. Scientific Reports. 2019 12; 9(1). doi: 10.1038/s41598-019-39092-7.

Clarke SE, Maler L. Feedback Synthesizes Neural Codes for Motion. Current Biology. 2017 5; 27(9). doi: 10.1016/j.cub.2017.03.068.

Coomber B, Edwards D, Jones SJ, Shackleton TM, Goldschmidt J, Wallace MN, Palmer AR. Cortical Inactivation by Cooling in Small Animals. Frontiers in Systems Neuroscience. 2011; 5. doi: 10.3389/fnsys.2011.00053.

Cunningham JP, Yu BM. Dimensionality reduction for large-scale neural recordings. Nat Neurosci. 2014 11; 17(11):1500–1509. doi: 10.1038/nn.3776.

Dai P, Huang H, Zhang L, He J, Zhao X, Yang F, Zhao N, Yang J, Ge L, Lin Y, Yu H, Wang J. A pilot study on transient ischemic stroke induced with endothelin-1 in the rhesus monkeys. Scientific Reports. 2017; 7. doi: 10.1038/SREP45097.

Darling WG, Pizzimenti MA, Rotella DL, Hynes SM, Ge J, Stilwell-Morecraft K, Morecraft RJ. Sensorimotor cortex injury effects on recovery of contralesional dexterous movements in Macaca mulatta. Exp Neurol. 2016 7; 281:37–52. doi: 10.1016/j.expneurol.2016.04.004.

DePaola BD. Op amps I. In: *Practical Analog, Digital, and Embedded Electronics for Scientists* IOP Publishing; 2020.doi: 10.1088/978-0-7503-3491-4ch12.

Dickey AS, Suminski A, Amit Y, Hatsopoulos NG. Single-Unit Stability Using Chronically Implanted Multielectrode Arrays. Journal of Neurophysiology. 2009; 102(2):1331–1339. doi: 10.1152/jn.90920.2008.

Elsayed GF, Lara AH, Kaufman MT, Churchland MM, Cunningham JP. Reorganization between preparatory and movement population responses in motor cortex. Nature Communications. 2016 12; 7(1):13239. doi: 10.1038/ncomms13239.

Fan J, Li Y, Fu X, Li L, Hao X, Li S. Nonhuman primate models of focal cerebral ischemia. Neural Regeneration Research. 2017; 12(2). doi: 10.4103/1673-5374.200815.

Ferrier D, Yeo GF. A record of experiments on the effects of lesions of different regions of the cerebral hemisphere. Philosophical Transactions of the Royal Society of London. 1884; 175(479-564).

Finnie JW, Blumbergs PC. Traumatic Brain Injury. Veterinary Pathology. 2002 11; 39(6). doi: 10.1354/vp.39-6-679.

Fish RM, Geddes LA. Conduction of electrical current to and through the human body: a review. Eplasty. 2009 10; 9:e44.

Fluri F, Schuhmann MK, Kleinschnitz C. Animal models of ischemic stroke and their application in clinical research. Drug Des Devel Ther. 2015; 9:3445–3454. doi: 10.2147/DDDT.S56071.

Fraser GW, Schwartz AB. Recording from the same neurons chronically in motor cortex. J Neurophysiol. 2012 4; 107(7):1970–1978. doi: 10.1152/jn.01012.2010.

Gallagher JJ, Svenson RH, Kasell JH, German LD, Bardy GH, Broughton A, Critelli G. Catheter Technique for Closed-Chest Ablation of the Atrioventricular Conduction System. New England Journal of Medicine. 1982 1; 306(4). doi: 10.1056/NEJM198201283060402.

Gallego JA, Perich MG, Chowdhury RH, Solla SA, Miller LE. Long-term stability of cortical population dynamics underlying consistent behavior. Nature Neuroscience. 2020 2; 23(2). doi: 10.1038/s41593-019-0555-4.

Ganguly K, Carmena JM. Emergence of a Stable Cortical Map for Neuroprosthetic Control. PLoS Biology. 2009 7; 7(7):e1000153. doi: 10.1371/journal.pbio.1000153.

Gerstein GL, Clark WA. Simultaneous Studies of Firing Patterns in Several Neurons. Science. 1964 3; 143(3612):1325–1327. doi: 10.1126/science.143.3612.1325.

Glees P, Cole J. Recovery of skilled motor functions after small repeated lesions of motor cortex in macaque. J Neurophysiol. 1950 3; 13(2):137–148.

Goldman JS, Tort-Colet N, di Volo M, Susin E, Bouté J, Dali M, Carlu M, Nghiem TA, Górski T, Destexhe A. Bridging Single Neuron Dynamics to Global Brain States. Frontiers in Systems Neuroscience. 2019 12; 13. doi: 10.3389/fnsys.2019.00075.

Golub MD, Sadtler PT, Oby ER, Quick KM, Ryu SI, Tyler-Kabara EC, Batista AP, Chase SM, Yu BM. Learning by neural reassociation. Nature neuroscience. 2018 4; 21(4):607–616. doi: 10.1038/s41593-018-0095-3.

Gould L, Kress S, Neudorf J, Gibb K, Persad A, Meguro K, Norton J, Borowsky R. An fMRI, DTI and Neurophysiological Examination of Atypical Organization of Motor Cortex in Ipsilesional Hemisphere Following Post-Stroke Recovery. Journal of Stroke and Cerebrovascular Diseases. 2021 3; 30(3). doi: 10.1016/j.jstrokecerebrovasdis.2020.105593.

Gulati T, Won SJ, Ramanathan DS, Wong CC, Bodepudi A, Swanson RA, Ganguly K. Robust neuroprosthetic control from the stroke perilesional cortex. J Neurosci. 2015 6; 35(22):8653–8661. doi: 10.1523/JNEUROSCI.5007-14.2015.

Hall JE, Hall ME. Guyton and Hall Textbook of Medical Physiology. In: *Guyton and Hall Textbook of Medical Physiology*, 14th ed. Philadelphia, PA: Elsevier; 2021.p. 613–623.

Higo N. Non-human Primate Models to Explore the Adaptive Mechanisms After Stroke. Frontiers in Systems Neuroscience. 2021 11; 15. doi: 10.3389/fnsys.2021.760311.

Hong G, Lieber CM. Novel electrode technologies for neural recordings. Nature Reviews Neuroscience. 2019 6; 20(6). doi: 10.1038/s41583-019-0140-6.

Horsley V, Schafer EA. A record of experiments upon the functions of the cerebral cortex. Philosophical Transactions of the Royal Society of London. 1888; 179B:1–45.

Jarrard LE. Use of excitotoxins to lesion the hippocampus: update. Hippocampus. 2002; 12(3):405–414. doi: 10.1002/hipo.10054.

Jun JJ, Steinmetz NA, Siegle JH, Denman DJ, Bauza M, Barbarits B, Lee AK, Anastassiou CA, Andrei A, Aydın Barbic M, Blanche TJ, Bonin V, Couto J, Dutta B, Gratiy SL, Gutnisky DA, Häusser M, Karsh B, Ledochowitsch P, et al. Fully integrated silicon probes for high-density recording of neural activity. Nature. 2017 11; 551(7679). doi: 10.1038/nature24636.

Kalaska JF. Emerging ideas and tools to study the emergent properties of the cortical neural circuits for voluntary motor control in non-human primates. F1000Research. 2019 5; 8. doi: 10.12688/f1000research.17161.1.

Khateeb K, Yao Z, Kharazia VN, Burunova EP, Song S, Wang R, Yazdan-Shahmorad A. A Practical Method for Creating Targeted Focal Ischemic Stroke in the Cortex of Nonhuman Primates. In: *2019 41st Annual International Conference of the IEEE Engineering in Medicine and Biology Society (EMBC)* IEEE; 2019. doi: 10.1109/EMBC.2019.8857741.

Kim CK, Adhikari A, Deisseroth K. Integration of optogenetics with complementary methodologies in systems neuroscience. Nat Rev Neurosci. 2017 3; 18(4):222–235. doi: 10.1038/nrn.2017.15.

Kleinschnitz C, Fluri F, Schuhmann M. Animal models of ischemic stroke and their application in clinical research. Drug Design, Development and Therapy. 2015 7; doi: 10.2147/DDDT.S56071.

Klomjai W, Katz R, Lackmy-Vallée A. Basic principles of transcranial magnetic stimulation (TMS) and repetitive TMS (rTMS). Annals of Physical and Rehabilitation Medicine. 2015 9; 58(4):208–213. doi: 10.1016/j.rehab.2015.05.005.

Kubota K. Motor cortical muscimol injection disrupts forelimb movement in freely moving monkeys. Neuroreport. 1996 10; 7(14):2379–2384.

Kuraoka M, Furuta T, Matsuwaki T, Omatsu T, Ishii Y, Kyuwa S, Yoshikawa Y. Direct Experimental Occlusion of the Distal Middle Cerebral Artery Induces High Reproducibility of Brain Ischemia in Mice. Experimental Animals. 2009; 58(1). doi: 10.1538/expanim.58.19.

Le W, Sayana P, Jankovic J. Animal Models of Parkinson's Disease: A Gateway to Therapeutics? Neurotherapeutics. 2014 1; 11(1). doi: 10.1007/s13311-013-0234-1.

Li N, Chen S, Guo ZV, Chen H, Huo Y, Inagaki HK, Chen G, Davis C, Hansel D, Guo C, Svoboda K. Spatiotemporal constraints on optogenetic inactivation in cortical circuits. eLife. 2019 11; 8. doi: 10.7554/eLife.48622.

Lind NM, Moustgaard A, Jelsing J, Vajta G, Cumming P, Hansen AK. The use of pigs in neuroscience: Modeling brain disorders. Neuroscience & Biobehavioral Reviews. 2007 1; 31(5). doi: 10.1016/j.neubiorev.2007.02.003.

Liu Y, Brincat SL, Miller EK, Hasselmo ME. A Geometric Characterization of Population Coding in the Prefrontal Cortex and Hippocampus during a Paired-Associate Learning Task. Journal of Cognitive Neuroscience. 2020 8; 32(8). doi: 10.1162/jocn{_}a{_}01569.

Lomber SG, Payne BR. Translaminar Differentiation of Visually Guided Behaviors Revealed by Restricted Cerebral Cooling Deactivation. Cerebral Cortex. 2000 11; 10(11). doi: 10.1093/cercor/10.11.1066.

Lomber SG, Payne BR, Horel JA. The cryoloop: an adaptable reversible cooling deactivation method for behavioral or electrophysiological assessment of neural function. Journal of Neuroscience Methods. 1999 1; 86(2). doi: 10.1016/S0165-0270(98)00165-4.

Long MA, Fee MS. Using temperature to analyse temporal dynamics in the songbird motor pathway. Nature. 2008 11; 456(7219). doi: 10.1038/nature07448.

Mancini R, Carter B, editors. Op Amps for Everyone. Third ed. Elsevier; 2009. doi: 10.1016/B978-1-85617-505-0.X0001-4.

Maynard EM, Nordhausen CT, Normann RA. The Utah Intracortical Electrode Array: A recording structure for potential brain-computer interfaces. Electroencephalography and Clinical Neurophysiology. 1997 3; 102(3). doi: 10.1016/S0013-4694(96)95176-0.

Mazurek KA, Schieber MH. Injecting Instructions into Premotor Cortex. Neuron. 2017 12; 96(6). doi: 10.1016/j.neuron.2017.11.006.

McNaughton BL, O'Keefe J, Barnes CA. The stereotrode: A new technique for simultaneous isolation of several single units in the central nervous system from multiple unit records. Journal of Neuroscience Methods. 1983 8; 8(4). doi: 10.1016/0165-0270(83)90097-3.

Morady F. Radio-Frequency Ablation as Treatment for Cardiac Arrhythmias. New England Journal of Medicine. 1999 2; 340(7). doi: 10.1056/NEJM199902183400707.

Murata Y, Higo N, Oishi T, Yamashita A, Matsuda K, Hayashi M, Yamane S. Effects of Motor Training on the Recovery of Manual Dexterity After Primary Motor Cortex Lesion in Macaque Monkeys. Journal of Neurophysiology. 2008 2; 99(2). doi: 10.1152/jn.01001.2007.

Musk E. An Integrated Brain-Machine Interface Platform With Thousands of Channels. Journal of Medical Internet Research. 2019 10; 21(10). doi: 10.2196/16194.

National Research Council (US) Committee for the Update of the Guide for the Care and Use of Laboratory Animals. Guide for the Care and Use of Laboratory Animals. Washington, D.C.: National Academies Press; 2011. doi: 10.17226/12910.

National Research Council (US) Committee on Guidelines for the Use of Animals in Neuroscience and Behavioral Research. Guidelines for the Care and Use of Mammals in Neuroscience and Behavioral Research. Washington, D.C.: National Academies Press; 2003. doi: 10.17226/10732.

Nikfarjam M, Muralidharan V, Christophi C. Mechanisms of Focal Heat Destruction of Liver Tumors. Journal of Surgical Research. 2005 8; 127(2):208–223. doi: 10.1016/j.jss.2005.02.009.

Nudo RJ, Friel KM. Cortical plasticity after stroke: Implications for rehabilitation. In: *Revue Neurologique*, vol. 155 Rev Neurol (Paris); 1999. p. 713–717.

Nudo RJ. Recovery after brain injury: mechanisms and principles. Front Hum Neurosci. 2013 12; 7:887. doi: 10.3389/fnhum.2013.00887.

Nudo RJ, Larson D, Plautz EJ, Friel KM, Barbay S, Frost SB. A squirrel monkey model of poststroke motor recovery. ILAR journal. 2003; 44(2):161–74. doi: 10.1093/ilar.44.2.161.

Obaid A, Hanna ME, Wu YW, Kollo M, Racz R, Angle MR, Müller J, Brackbill N, Wray W, Franke F, Chichilnisky EJ, Hierlemann A, Ding JB, Schaefer AT, Melosh NA. Massively parallel microwire arrays integrated with CMOS chips for neural recording. Science Advances. 2020 3; 6(12). doi: 10.1126/sciadv.aay2789.

Rajalingham R, Sorenson M, Azadi R, Bohn S, DiCarlo JJ, Afraz A. Chronically implantable LED arrays for behavioral optogenetics in primates. Nature Methods. 2021 8; doi: 10.1038/s41592-021-01238-9.

Ramanathan DS, Guo L, Gulati T, Davidson G, Hishinuma AK, Won SJ, Knight RT, Chang EF, Swanson RA, Ganguly K. Low-frequency cortical activity is a neuromodulatory target that tracks recovery after stroke. Nat Med. 2018 8; 24(8):1257–1267. doi: 10.1038/s41591-018-0058-y.

Rasmussen RG, Schwartz A, Chase SM. Dynamic range adaptation in primary motor cortical populations. eLife. 2017 4; 6. doi: 10.7554/eLife.21409.

Rios G, Lubenov EV, Chi D, Roukes ML, Siapas AG. Nanofabricated Neural Probes for Dense 3-D Recordings of Brain Activity. Nano Letters. 2016 11; 16(11):6857–6862. doi: 10.1021/acs.nanolett.6b02673.

Rousche PJ, Normann RA. Chronic recording capability of the Utah Intracortical Electrode Array in cat sensory cortex. Journal of Neuroscience Methods. 1998 7; 82(1). doi: 10.1016/S0165-0270(98)00031-4.

Rousche PJ, Normann RA. Chronic intracortical microstimulation (ICMS) of cat sensory cortex using the Utah intracortical electrode array. IEEE Transactions on Rehabilitation Engineering. 1999 3; 7(1). doi: 10.1109/86.750552.

Rumajogee P, Bregman T, Miller SP, Yager JY, Fehlings MG. Rodent Hypoxia–Ischemia Models for Cerebral Palsy Research: A Systematic Review. Frontiers in Neurology. 2016 4; 7. doi: 10.3389/fneur.2016.00057.

Sadtler PT, Quick KM, Golub MD, Chase SM, Ryu SI, Tyler-Kabara EC, Yu BM, Batista AP. Neural constraints on learning. Nature. 2014 8; 512(7515):423–426. doi: 10.1038/nature13665.

Scheinman MM. Catheter-Induced Ablation of the Atrioventricular Junction to Control Refractory Supraventricular Arrhythmias. JAMA: The Journal of the American Medical Association. 1982 8; 248(7). doi: 10.1001/jama.1982.03330070039027.

Schieber MH, Poliakov AV. Partial inactivation of the primary motor cortex hand area: effects on individuated finger movements. J Neurosci. 1998 11; 18(21):9038–9054.

Shenoy KV, Kao JC. Measurement, manipulation and modeling of brain-wide neural population dynamics. Nature communications. 2021; 12(1):633. doi: 10.1038/s41467-020-20371-1.

Sherrington CS. Further experimental note on the correlation of action of antagonistic muscles. Proc Roy Roc. 1893; 53:407–420.

Shivkumar K. Catheter Ablation of Ventricular Arrhythmias. New England Journal of Medicine. 2019 4; 380(16). doi: 10.1056/NEJMra1615244.

Slonina ZA, Poole KC, Bizley JK. What can we learn from inactivation studies? Lessons from auditory cortex. Trends in Neurosciences. 2022 1; 45(1):64–77. doi: 10.1016/j.tins.2021.10.005.

Sporns O. Connectome Networks: From Cells to Systems. In: *Micro-, Meso- and Macro-Connectomics of the Brain*, 1 ed. Springer; 2016.doi: 10.1007/978-3-319-27777-6{_}8.

Steigerwald F, Matthies C, Volkmann J. Directional Deep Brain Stimulation. Neurotherapeutics. 2019 1; 16(1). doi: 10.1007/s13311-018-0667-7.

Steinmetz NA, Aydin C, Lebedeva A, Okun M, Pachitariu M, Bauza M, Beau M, Bhagat J, Böhm C, Broux M, Chen S, Colonell J, Gardner RJ, Karsh B, Kloosterman F, Kostadinov D, Mora-Lopez C, O'Callaghan J, Park J, Putzeys J, et al. Neuropixels 2.0: A miniaturized high-density probe for stable, long-term brain recordings. Science. 2021 4; 372(6539). doi: 10.1126/science.abf4588.

Sternson SM, Roth BL. Chemogenetic tools to interrogate brain functions. Annu Rev Neurosci. 2014; 37:387–407. doi: 10.1146/annurev-neuro-071013-014048.

Vaidya AR, Pujara MS, Petrides M, Murray EA, Fellows LK. Lesion Studies in Contemporary Neuroscience. Trends Cogn Sci. 2019 8; 23(8):653–671. doi: 10.1016/j.tics.2019.05.009.

Vaidya M, Dickey A, Best MD, Coles J, Balasubramanian K, Suminski AJ, Hatsopoulos NG. Ultra-long term stability of single units using chronically implanted multielectrode arrays. In: *2014 36th Annual International Conference of the IEEE Engineering in Medicine and Biology Society, EMBC 2014* Institute of Electrical and Electronics Engineers Inc.; 2014. p. 4872–4875. doi: 10.1109/EMBC.2014.6944715.

Virtanen P, Gommers R, Oliphant TE, Haberland M, Reddy T, Cournapeau D, Burovski E, Peterson P, Weckesser W, Bright J, van der Walt SJ, Brett M, Wilson J, Millman KJ, Mayorov N, Nelson ARJ, Jones E, Kern R, Larson E, Carey CJ, et al. SciPy 1.0: fundamental algorithms for scientific computing in Python. Nature Methods. 2020 3; 17(3):261–272. doi: 10.1038/s41592-019-0686-2.

Vogt N. Optogenetic inhibition. Nature Methods. 2020 1; 17(1). doi: 10.1038/s41592-019-0712-4.

Vyas S, O'Shea DJ, Ryu SI, Shenoy KV. Causal Role of Motor Preparation during Error-Driven Learning. Neuron. 2020 4; 106(2):329–339. doi: 10.1016/j.neuron.2020.01.019.

Watson BD, Dietrich WD, Busto R, Wachtel MS, Ginsberg MD. Induction of reproducible brain infarction by photochemically initiated thrombosis. Ann Neurol. 1985 5; 17(5):497–504. doi: 10.1002/ana.410170513.

Weiss JM, Flesher SN, Franklin R, Collinger JL, Gaunt RA. Artifact-free recordings in human bidirectional brain–computer interfaces. Journal of Neural Engineering. 2019 2; 16(1). doi: 10.1088/1741-2552/aae748.

Wise KD, Angell JB, Starr A. An Integrated-Circuit Approach to Extracellular Microelectrodes. IEEE Transactions on Biomedical Engineering. 1970 7; BME-17(3). doi: 10.1109/TBME.1970.4502738.

Woods AJ, Antal A, Bikson M, Boggio PS, Brunoni AR, Celnik P, Cohen LG, Fregni F, Herrmann CS, Kappenman ES, Knotkova H, Liebetanz D, Miniussi C, Miranda PC, Paulus W, Priori A, Reato D, Stagg C, Wenderoth N, Nitsche MA. A technical guide to tDCS, and related non-invasive brain stimulation tools. Clinical Neurophysiology. 2016 2; 127(2):1031–1048. doi: 10.1016/j.clinph.2015.11.012.

Wurtz RH, Goldberg ME. Activity of superior colliculus in behaving monkey. IV. Effects of lesions on eye movements. J Neurophysiol. 1972 7; 35(4):587–596. doi: 10.1152/jn.1972.35.4.587.

Yu BM, Cunningham JP, Santhanam G, Ryu SI, Shenoy KV, Sahani M. Gaussian-Process Factor Analysis for Low-Dimensional Single-Trial Analysis of Neural Population Activity. Journal of Neurophysiology. 2009 7; 102(1):614–635. doi: 10.1152/jn.90941.2008.

Zeiler SR, Hubbard R, Gibson EM, Zheng T, Ng K, O'Brien R, Krakauer JW. Paradoxical Motor Recovery From a First Stroke After Induction of a Second Stroke: Reopening a Postischemic Sensitive Period. Neurorehabil Neural Repair. 2015 12; doi: 10.1177/1545968315624783.

Zhang T, Pan N, Wang Y, Liu C, Hu S. Transcranial Focused Ultrasound Neuromodulation: A Review of the Excitatory and Inhibitory Effects on Brain Activity in Human and Animals. Frontiers in Human Neuroscience. 2021 9; 15. doi: 10.3389/fnhum.2021.749162.

Appendix 1

Design Considerations

A technique that combines electrophysiology with permanent inactivation of neuronal activity will meet three main design considerations:

1. stable electrophysiology pre- and post-inactivation
2. ability to localize and control the size of the inactivation
3. cross-compatibility

Stable electrophysiology pre- and post-inactivation

Stable electrophysiological recordings over time allow baseline neuronal activity to be directly compared to the activity recorded after inactivation. This comparison would capture the acute effects of inactivation on both the neuronal activity and the animal's behavior, as well as long term changes associated with behavioral recovery. As any physical disruption of the microelectrode array would affect the stability of the recordings and negatively impact pre-post comparisons, it is essential to avoid physical disruption of the array from surgical procedures and minimize additional implanted devices or cannulae, which may act as routes for infection to enter the brain.

Ability to localize and control the size of the inactivation

Prior studies suggest that after inactivating neuronal activity in a region, compensatory neuronal changes will happen in the area closely surrounding that region ***Nudo and Friel*** (***1999***); ***Nudo*** (***2013***); ***Gould et al.*** (***2021***). In order to ensure that the microelectrode array is recording from this peri-inactivation area, the location of the inactivation (both point of origin and extent) must be precisely controlled. The microelectrode array should be close enough to the inactivation to record from the peri-inactivation area, but the inactivation area should not be so large or so close to the microelectrode array that it completely encompasses the array's recording area. If the microelectrode array only records from the inactivated area (and therefore inactivated neurons), the recordings will only verify that the inactivation method worked and will not enable further scientific questions.

While some methods do allow for inactivation at a certain point in space, the effects can spread quite far or uncontrollably from that point due to various biological mechanisms. These mechanisms can include pharmacological diffusion and continued neuronal death after ischemic injury ***Kubota*** (***1996***); ***Schieber and Poliakov*** (***1998***); ***Jarrard*** (***2002***). This spread would not allow control over how much of the recording area of the microelectrode array was in the peri-inactivation region or the inactivation region itself. Therefore, both precision in localizing the inactivation and control over its spread are required.

Finally, an inactivation technique should enable studying both the effects of inactivation on neuronal activity and how neuronal activity changes when behavior recovers following inactivation ***Slonina et al.*** (***2022***). This requires the inactivation to be small enough for the animal to recover ***Nudo et al.*** (***2003***); ***Wurtz and Goldberg*** (***1972***); ***Glees and Cole*** (***1950***). Inactivating a small region may enable investigation about the causal role of the inactivated neurons while avoiding confounding effects across multiple, broad systems.

Cross-compatibility

Ideally, a technique that combines electrophysiology with inactivation could be used in any area of cortex, with any multielectrode probe, and in several species in order to enable causal investigation in a large variety of contexts. Flexibility over the cortical area studied and the multielectrode probes used will enable easy adoption into existing neuroelectrophysiology recording setups across many neuroscience contexts. Compatibility with a variety of animal models will further increase the technique's utility. Electrophysiology studies and animal models of brain disease have spanned many species, from rodents to large animals ***Rousche and Normann*** (***1998***, 1999); ***Le et al.*** (***2014***); ***Finnie and Blumbergs*** (***2002***); ***Lind et al.*** (***2007***); ***Kleinschnitz et al.*** (***2015***); ***Fan et al.*** (***2017***); ***Nudo et al.*** (***2003***). While each species offers

its own experimental benefits and limitations, the majority of tools and techniques in this space have been developed for rodents. Rather than being limited to rodents, an inactivation technique would ideally also be compatible with large animals such as rhesus macaques, due to their dexterity, ability to perform complex movements, and extensive history in electrophysiology studies of motor control ***Higo*** (***2021***).

Appendix 2

Manipulations are temporary inactivations of neuronal activity, while terminations are permanent inactivations. There are several existing methods for achieving a manipulation or a termination. Although each existing method has its own strengths, none is able to meet all three of the previously mentioned design considerations of: stable electrophysiology pre- and post-inactivation, ability to localize and control the size of the inactivation, and cross-species and large-animal compatibility.

Existing Manipulation Methods

Existing temporary inactivation methods include intracortical microstimulation, optogenetics, pharmacology, transcranial stimulation, cooling loops, and chemogenetics.

Intracortical microstimulation, where small pulses of current are applied to cortex, can be used to temporarily disrupt neuronal activity ***Churchland and Shenoy*** (***2007***); ***Mazurek and Schieber*** (***2017***); ***Vyas et al.*** (***2020***). It can be performed using the same neuroelectrophysiology electrodes being used to record, requiring no additional surgical access ***Weiss et al.*** (***2019***). However, it can be challenging to sustain a behavioral effect with continuous microstimulation.

Optogenetic silencing can inactivate an area either by using an inhibitory step-function opsin ***Berndt et al.*** (***2014***); ***Kim et al.*** (***2017***) or by activating a local inhibitory circuit ***Vogt*** (***2020***); ***Li et al.*** (***2019***). Long-term local silencing of a region of cortex could be achieved with continued illumination by a fiber or a chronically implanted array of light-emitting diodes ***Rajalingham et al.*** (***2021***). However, challenges with this approach include the need to develop a head-mounted, battery powered light delivery system for multi-day delivery of light, the lack of rhesus compatible constructs, and difficulty integrating illumination with simultaneous chronic neuroelectrophysiology.

Pharmacological agents like muscimol and lidocaine can also be used for transient inactivation ***Kubota*** (***1996***); ***Schieber and Poliakov*** (***1998***); ***Clarke and Maler*** (***2017***). A pathway is required to deliver the agent to the appropriate area of cortex. If this pathway is chronically implanted (e.g., a cannula), then it can be placed somewhat precisely near the microelectrode array, but it would act as a potential route for a local infection, which may cause swelling of the tissue and lead to partial displacement of the array or other medical complications. An alternative is to inject the agent though a burr hole created only when lesioning is desired, though it may be difficult to localize the placement of the burr hole within the immediate area of the microelectrode array. Controlling spread of pharmacological agents is also difficult, especially for drugs with low molecular weight. The effects of pharmacological agents will fluctuate over space and time as they diffuse through the tissue and begin to be cleared or metabolized.

Non-invasive methods like transcranial magnetic stimulation (TMS), transcranial direct stimulation (tDCS), and transcranial focal ultrasound lead to very temporary inactivation ***Klomjai et al.*** (***2015***); ***Woods et al.*** (***2016***); ***Zhang et al.*** (***2021***). In addition to the short timescale of these inactivations, their effects are dispersed as the signal must travel through the skull. These methods provide neither the spatial resolution nor the temporal duration needed for probing local neuronal circuitry.

Cooling loops are implanted devices that effectively silence nearby cells by affecting action potential generation, axon conduction velocity, and synaptic transmission ***Lomber et al.*** (***1999***); ***Lomber and Payne*** (***2000***); ***Long and Fee*** (***2008***); ***Chen et al.*** (***2020***). These devices would be implanted at the same time as the microelectrode array, and they would not require surgical access to use. However, cooling cannot easily be maintained across days while the animal is in its home environment. In addition to damaging valuable nearby tissue during the implant surgery and introducing another foreign body, cooling inactivates on the scale of millimeters, limiting the ability to titrate the size of the inactivation any smaller ***Coomber et al.*** (***2011***).

A region of cortex can also be temporarily inactivated with chemogenetic silencing, using chemically activated proteins to inhibit neuronal activity ***Sternson and Roth*** (***2014***). The chemical is injected intravenously, so the process would not disrupt the placement of the microelectrode array. As with optogenetic silencing, chemogenetics would require the development of rhesus compatible constructs. Additionally,

chronic inactivation over days may be logistically challenging, as the half life of CNO is on the order of hours.

Existing Termination Methods

Existing termination methods include physical damage, endovascular occlusion, Rose Bengal mediated photothrombosis, and chemical lesioning.

There are several well established techniques for mechanically damaging a small area of cortex to create a lesion, including blade lesioning ***Horsley and Schafer*** (***1888***); ***Sherrington*** (***1893***), vacuum aspiration ***Darling et al.*** (***2016***), vascular cauterization ***Nudo et al.*** (***2003***), and vascular ligation ***Rumajogee et al.*** (***2016***). All of these techniques require surgical access to cortex, which would likely disrupt an existing implanted microelectode array. Additionally, the sedation necessary for the surgery would prevent behavioral testing on the day of the lesion, precluding measurements of acute inactivation. Further, these techniques often create large lesions, and do not offer sub-millimeter precision.

Endovascular techniques are commonly used as models of stroke. For example, endovascular physical occlusion of the middle cerebral artery (MCA) of one hemisphere is a common rodent model of stroke ***Fluri et al.*** (***2015***), but it is challenging to precisely control the extent of cortical damage. MCA occlusion could cause indiscriminate injury to a large regions of cortex, due to continued, widespread neuronal death after the occlusion. It could potentially damage the area in which the microelectrode array is implanted, preventing meaningful recordings. As one descends into smaller branches of the MCA, survivability, localization, and reproducibility of ischemic results improve ***Kuraoka et al.*** (***2009***); ***Clark et al.*** (***2019***), but it is technically challenging to be precise with the occlusion without coming close to the implanted array, again risking disrupting the implantation site.

Another endovascular technique is photothrombosis, which does not require an additional surgery to implement, limiting disruption of the microelectrode array. ***Gulati et al.*** (***2015***); ***Ramanathan et al.*** (***2018***); ***Khateeb et al.*** (***2019***). This approach uses rose bengal, a photosenstive dye, injected intravenously into the circulatory system. When 561nm green light is shined over a blood vessel, the dye undergoes a local conformational change and generates singlet oxygen, damaging arterial endothelial cells and initiating the clotting cascade–resulting in damage resembling an ischemic stroke ***Watson et al.*** (***1985***); ***Carmichael*** (***2005***). This approach can be used to deliver a well-localized lesional boundary. In rodents, this can be done entirely non-invasively because green light penetrates through the thin layer of skull. In larger animals, a method of light delivery is needed. If an optical fiber is chronically implanted at the time of electrode array insertion, light can be delivered without surgery and lesions can be made without disrupting the array, but this chronically implanted fiber may act as a route for infection. Alternatively, the fiber could be placed though a burr hole made at the time of the lesion, but this may compromise localization accuracy like other burr-hole techniques.

Chemical lesioning is done by injecting a damaging chemical into the cortical region. These chemicals can be excitotoxic pharmacologic agents like ibotenic acid that selectively and directly damage neuronal cell bodies ***Murata et al.*** (***2008***), or they can be vasoconstrictors like endothelin-1 that create anoxic cortical injury ***Dai et al.*** (***2017***). These chemicals have the same potential drawbacks of other injection-based methods: either a permanent pathway is added to allow precise injection in the area of the microelectrode array, creating a route for infection, or injection is done through a burr hole, making it difficult to localize to the region of the array and disrupting experimental continuity. It is also difficult to control the spread of the chemicals, preventing precision in lesion extent.

Supplementary Material

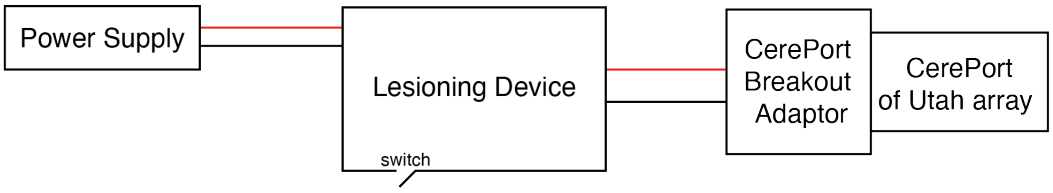

Figure S1. Connection diagram of the experimental setup for creating electrolytic lesions.

Date	Animal	Age	Current (uA)	Duration (min)	Voltage Related Notes
180702	Sheep	Adult	510	20	no current delivered (faulty setup)
180702	Sheep	Adult	480	20	90V (etching; less than 30s), 22V
180702	Sheep	Adult	250	10	90V (etching; few seconds), 16V
180716	Pig	Juvenile	180	2	immediate voltage drop
180716	Pig	Juvenile	180	2	immediate voltage drop
180716	Pig	Juvenile	180	2	immediate voltage drop
180716	Pig	Juvenile	180	2	immediate voltage drop
180716	Pig	Juvenile	180	2	immediate voltage drop
180716	Pig	Juvenile	180	2	immediate voltage drop
180727	Pig	Juvenile	180	2.2	<15V
180727	Pig	Juvenile	N/A	5.5	N/A
180727	Pig	Juvenile	180	2	15V average
180727	Pig	Juvenile	180	2	<15V
180727	Pig	Juvenile	N/A	6	N/A
180727	Pig	Juvenile	180	1	<15V
180727	Pig	Juvenile	180	1	<15V
180727	Pig	Juvenile	180	1	<15V
180727	Pig	Juvenile	180	1	<15V

Table S1. Lesion parameters used for *ex vivo* testing. Voltage was monitored with a voltmeter during lesioning, and notes were collected about the voltage. Tests that were performed solely to understand the effect of impacting and removing the microelectrode array without passing any current to create an electrolytic lesion are indicated with N/A for the current value. One *ex vivo* brain was used for all testing on 180702, and two *ex vivo* brains were used on each of the other two dates.

Date	Animal	Sex	Age (wks)	Current (uA)	Duration (min)	Voltage Related Notes
190215	Pig	F	13	150	1	voltage railed
190215	Pig	F	13	150	1	<15V
190215	Pig	F	13	240	1	voltage railed
190215	Pig	F	13	240	1	<15V
190215	Pig	F	13	240	2	<15V
190215	Pig	F	13	150	2	<15V
190215	Pig	F	13	150	5	<15V
190215	Pig	F	13	185	10	<15V
190326	Pig	F	10	N/A	N/A	N/A
190326	Pig	F	10	100	1	<15V, briefly 30V, <15V
190326	Pig	F	10	100	0.5	<15V
190326	Pig	F	10	100	0.25	voltage railed
190326	Pig	F	10	100	1	<15V
190326	Pig	F	10	100	1	<15V
190326	Pig	F	10	50	0.5	<15V
190326	Pig	F	10	50	1	<15V
190326	Pig	F	10	150	0.5	<15V
190326	Pig	F	10	N/A	N/A	N/A
190416	Pig	F	16	50	0.5	<15V
190416	Pig	F	16	50	1	<15V
190416	Pig	F	16	N/A	N/A	N/A
190416	Pig	F	16	100	0.5	<15V
190416	Pig	F	16	100	1	voltage railed
190416	Pig	F	16	50	0.5	<15V
190416	Pig	F	16	N/A	N/A	N/A
190416	Pig	F	16	50	1	<15V
190416	Pig	F	16	100	0.5	<15V
190416	Pig	F	16	100	1	<15V
190513	Pig	F	10	50	1	<15V
190513	Pig	F	10	50	1	<15V
190513	Pig	F	10	N/A	N/A	N/A
190513	Pig	F	10	150	2	voltage railed
190513	Pig	F	10	150	1	<15V
190513	Pig	F	10	N/A	N/A	N/A
200203	Pig	F	9	450	0.2	
200203	Pig	F	9	450	0.5	
200203	Pig	F	9	450	0.2	
200203	Pig	F	9	450	0.2	
200203	Pig	F	9	450	0.2	
200203	Pig	F	9	450	0.2	
200203	Pig	F	9	450	0.2	voltage railed
200203	Pig	F	9	450	0.2	
200203	Pig	F	9	350	0.2	<15V

Table S2. Lesion parameters used for *in vivo* testing. Voltage was monitored with a voltmeter during lesioning, and notes were collected about the voltage. Tests that were performed solely to understand the effect of impacting and removing the microelectrode array without passing any current to create an electrolytic lesion are indicated with N/A for the current value. One animal was used for all testing on a given date.